QUENCHING OF HEATED METAL SURFACE USING WATER SPRAY

M. Mousa

Department of Mechanical Power Engineering, Faculty of Engineering, Menoufia University, Shebin El-kom, Egypt.

ABSTRACT

Transient cooling heat transfer experiments of a heated metal specimen with impinging spray water have been conducted. The measurement of water spray characteristics such as droplet size and impinging velocity at various heights downstream of a spray nozzle are conducted using a Phase Doppler Particle Analyzer (PDPA). Full-cone nozzles with orifice diameter from 1.4 to 2.3 mm are used with an injection pressure of water ranging from 0.1 to 0.4 MPa. The distributions of droplet size, impinging velocity and water mass velocity are measured from 0 to 0.5 m downstream of the spray nozzle. A copper specimen of dimensions 100×100×30 mm was used as a heat transfer target. The specimen was heated up to 800 °C and exposed horizontally to the water spray. The spray nozzle was set up vertically above the target and the spray angle was traversed from 0 to 60° from the vertical direction. The change of temperature with time at two positions inside the metal specimen is recorded with a data acquisition system. The first position is at 3 mm from the upper surface and the second at the center of specimen. The surface temperature and heat flux is estimated numerically by solving the inverse heat conduction model. An iteration method is presented to estimate the temperature distribution inside the specimen at time interval of 10^{-5} sec. The evaporation heat transfer coefficient was assumed in order to obtain the temperature distribution inside the specimen and readjusted to give a temperature difference of 0.01 °C between the measured and estimated values. The boiling curves from the transient cooling process at different spray characteristics were obtained. The effects of the spray characteristics and spray angles on surface heat flux are investigated. The cooling time is shorter at spray impinging angle $\alpha = 30°$ than that with vertical spray at $We \leq 10$ and mass velocity ≤ 0.143 kg/m^2. s. The mass velocity of water is the most dominant parameter in the film-boiling region. The droplet size and impinging velocity have little effects at high surface temperature, and the evaporation heat transfer decreases with increasing the spray angle from vertical. A generalized correlation of evaporation heat transfer of film boiling between horizontal surface and vertical or inclined impinging water sprays has been obtained.

Keywords: Quench cooling, Inverse heat conduction, Spray cooling, Evaporation heat flux, Film boiling.

INTRODUCTION

Transient cooling of a high temperature metal surface with a water spray is found in several industrial applications. The production of carbon-steel, copper, aluminum and other alloys having desired mechanical and metallurgical properties require accurate temperature control during processing. The cooling of a plate, hot strip mill or flange beam mill in a continuous casting machine is mainly a transient cooling process of an atmospheric water spray systems. To obtain desired properties of metal products with water spray, it is important to know the heat transfer mechanism of impinging water spray upon a heated metal surface and the effects of spray parameters upon the surface heat flux. In the hot strip mill applications, the strip temperature is in excess of 800 °C. In this range of surface temperature, the wetting of the surface with water is very difficult. This is the range of boiling known as the stable film boiling, where a stable vapor layer insulates the surface from the water spray. The film boiling heat transfer is influenced by the droplet size, impinging velocity, mass velocity, spray angle and surface roughness. Yet, comprehensive quantitative information regarding the heat removal rate provided by such water sprays is not readily available in the literature.

In the conventional quenching process, the heat transfer surface is normally covered by a thin oxide film. The surface oxide film actually changes the surface roughness. Pais *et al.* [1] experimentally investigated the effect of surface texture (surface roughness) on the bubble diameter, vapor entrapment and bubble departure characteristics at low surface superheating. Sabry *et al.* [2] also examined the effect of surface roughness on evaporation heat flux from sprayed water droplets of transient cooling process at high surface superheating. They concluded that the effect of surface roughness is less important in the film-boiling region, but has obvious effect in the transition and nucleate boiling regions. Horsky *et al.* [3] performed a comprehensive study of heat transfer cooling of a surface using a water-air nozzle. The effect of droplet size and impinging velocity were investigated, finer droplets cause a better heat transfer. Ito et al. [4, 5] and Mousa [6, 7] summarized numerous reports which are related to transient cooling of heated metal surface with impinging water spray. The survey indicated that the effect of mass velocity of water is a very important parameter in transient cooling processes. The previous tests compare different spray nozzles and spray parameters under different test conditions. The aim of the tests is to get an understanding of the mechanism of heat transfer during quenching with water spray as well as providing data for the process engineer, who has to design an efficient cooling system [8]. Though literature offers a lot of tests, no clear picture could be obtained until today, which includes all the parameters influencing the heat transfer of spray cooling process. Furthermore, additional comprehensive heat transfer experiments are necessary to investigate and explain the quenching cooling process with water spray at different spray parameters and spray angles.

The objective of the present study is to investigate experimentally the effect of spray characteristics and impinging spray angle on evaporation heat flux of transient quench cooling. Precise details of the effect of water spray characteristics such as droplet size and impinging velocity and water mass velocity upon the heat transfer surface were aimed. Also the effect of spray impinging angle on the evaporation heat flux were investigated. A generalized correlation of evaporation heat flux in film boiling region during transient quenching processes is also one of the targets of this work.

EXPERIMENTAL ARRANGEMENT

The experimental setup serves two groups of experiments. The first group is for measuring the spray characteristics such as the distribution of droplet size and velocities within the water spray cone using Phase-Doppler Particle Analyzer (PDPA). The impinging mass velocities of water upon the heated surface were measured. The second group is concerned with recording the temperature-time curves of the transient cooling process inside a copper specimen using a data acquisition system. The k-type thermocouples with outside diameter of 1 mm are used to measure all of the temperatures inside the metal specimen and send it to a personal computer. The error in temperature measurement is within ± 0.1 °C.

MEASUREMENTS OF SPRAY CHARACTERISTICS

Using different spray nozzles and injection pressure controls the spray characteristics such as droplet size, impinging velocity and mass velocity of water. A full description of the measured spray characteristics using PDPA at various heights downstream of the spray nozzle and radial direction from the spray centerline has been given in reference [9]. However, a brief description of measuring the droplet size distribution and velocity at 0.5 *m* downstream of the spray nozzle is given here. The schematic of spray test facility for measuring droplet size and velocity is shown in Figure 1.

Water spray is formed by droplets of different sizes resulting from the fast disintegration of an unstable liquid sheet from the spray nozzle [10,11]. The spray nozzle is fed by water from a pumping system at an adjustable injection pressure from 0.1 to 0.4 MPa. The water mass flow rate, temperature and pressure measurements are made just upstream of the spray nozzle. The spray nozzles are manufactured by Kyoritsu Alloy C. Ltd. The spray nozzle is mounted on a vertical translator that held by a manifold in vertical position. The nozzle and resulting water spray are translated both vertically and horizontally relative to the focus of two laser beams that remain stationary. The drain pool and spray nozzle are mounted on a displacement table that can traverse the centerline of the water spray in the radial direction out of the laser focus from 0 to 120 mm. The spray nozzle is set on a translator enabling measurement heights from 0 to 1 m. Using these two movements; the spray cone can be investigated in two directions. Prior to each experiment, the focus of the two laser beams was adjusted at the centerline downstream of spray nozzle. The vertical position of the spray nozzle from the focus of the laser beams is also adjusted at 0.5 m. The radial distance of the spray centerline could be easily controlled by using the displacement table.

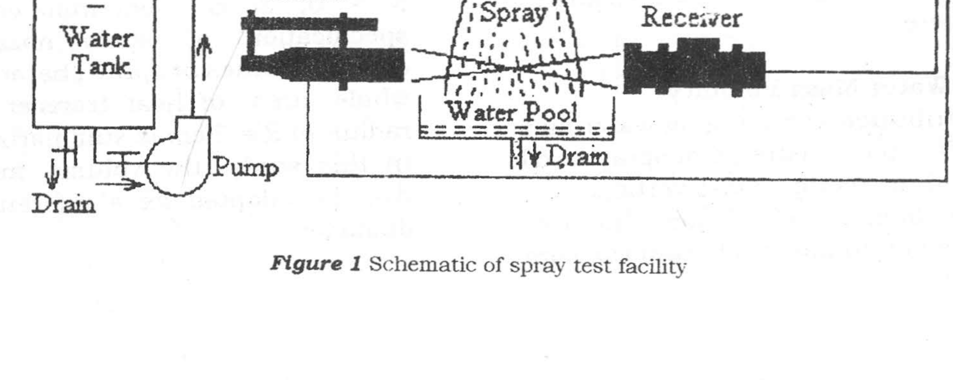

Figure 1 Schematic of spray test facility

Distribution of Droplet Size and Velocity

The Phase Doppler Particle Analyzer gives directly a local measurement of spray droplet size and velocity. At each measurement point, the data were collected over a period of 10000 samples. The distribution curves of size and velocity gives an accurate description of the spray structure. A sample of size and velocity distribution curves and mean value of droplet diameter and velocity are illustrated in Figure 2.

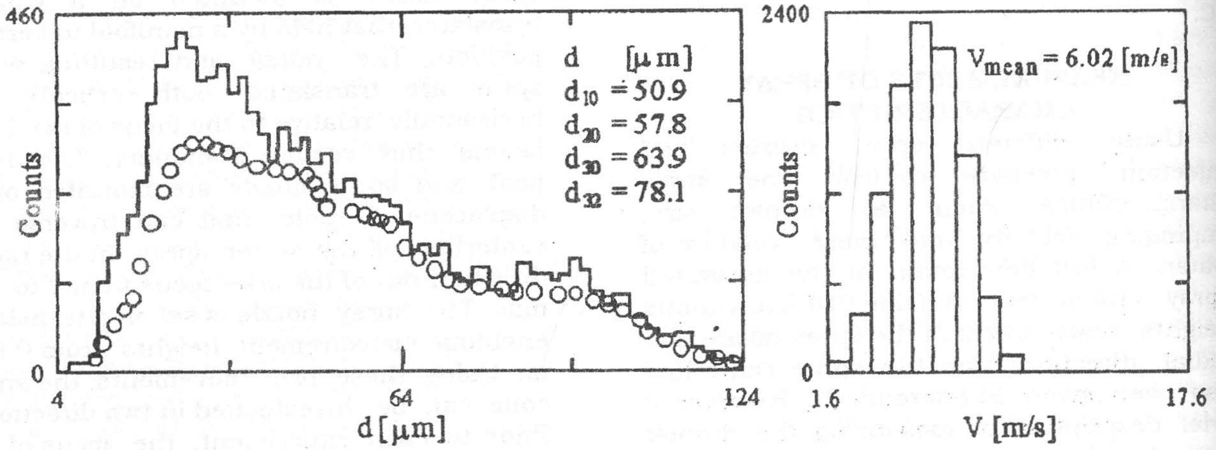

Figure 2 Sample of droplet size and velocity distribution

Figure 3 shows the evaluation of droplet size at height 0.5 m downstream of the spray nozzle and various radial distances from the spray centerline. For nozzles JN3 and JN4, the droplet size slightly increases with increasing the radial distance. But for nozzle JN5 and JN6, the change of droplet size is negligible at spray pressure up to 0.2 MPa. Obviously, the droplet size decreases with increasing spray pressure. The distribution of droplet velocity with radial distance is shown in Figure 4. The droplet velocity decreases with increasing the radial distance and increases with increasing the spray pressure.

Impinging Water Mass Velocity

The distribution of impinging water mass velocity at 0.5 m downstream of spray nozzle is conducted by using a glass vertical tubes with inside diameter of 10 mm. The tubes are arranged at 30 mm pitch from the spray centerline. The droplets were collected in a certain period of time. The average of 3 experimental data at the above water spray condition is taken as the nominal mass velocity of water, $\dot{m}$. Figure 5 shows the variation of impinging water mass velocity upon the surface with the radial distance R. From Figure 5 at R = -6 to 6 cm for all nozzles, the distribution of water mass velocity on this area is very small and quite uniform. The average values of droplet size, droplet velocity and water mass velocity are taken as the average value of three values at R = 0, 3, 6 cm from centerline. The specification of spray nozzles and the average values of spray characteristic over a whole area of heat transfer surface with radius of R = 5 cm is summarized in Table 1. In this study, the volume mean diameter, d_{30}, is adopted as a reference of droplet diameter.

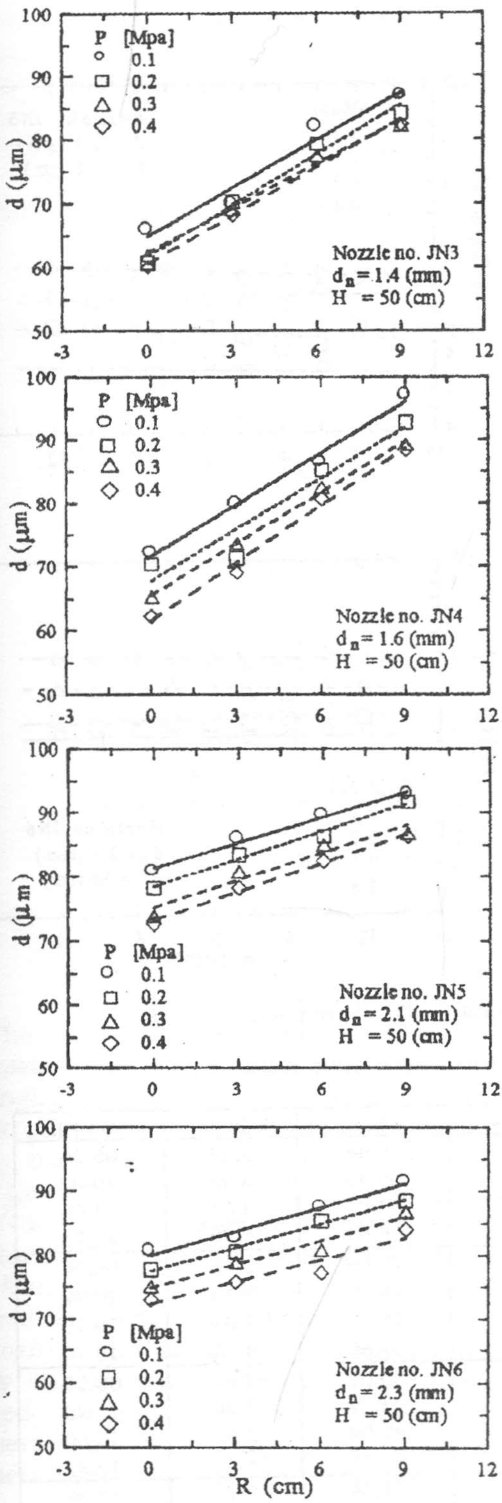

Figure 3 Droplet size radial distribution.

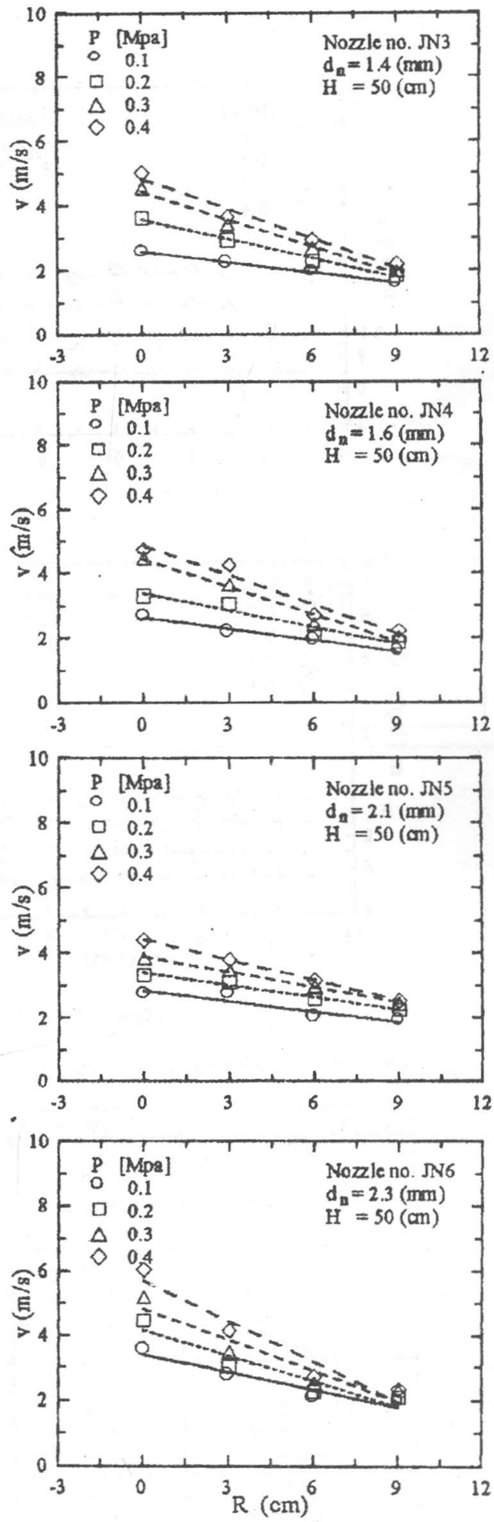

Figure 4 Droplet size radial distribution.

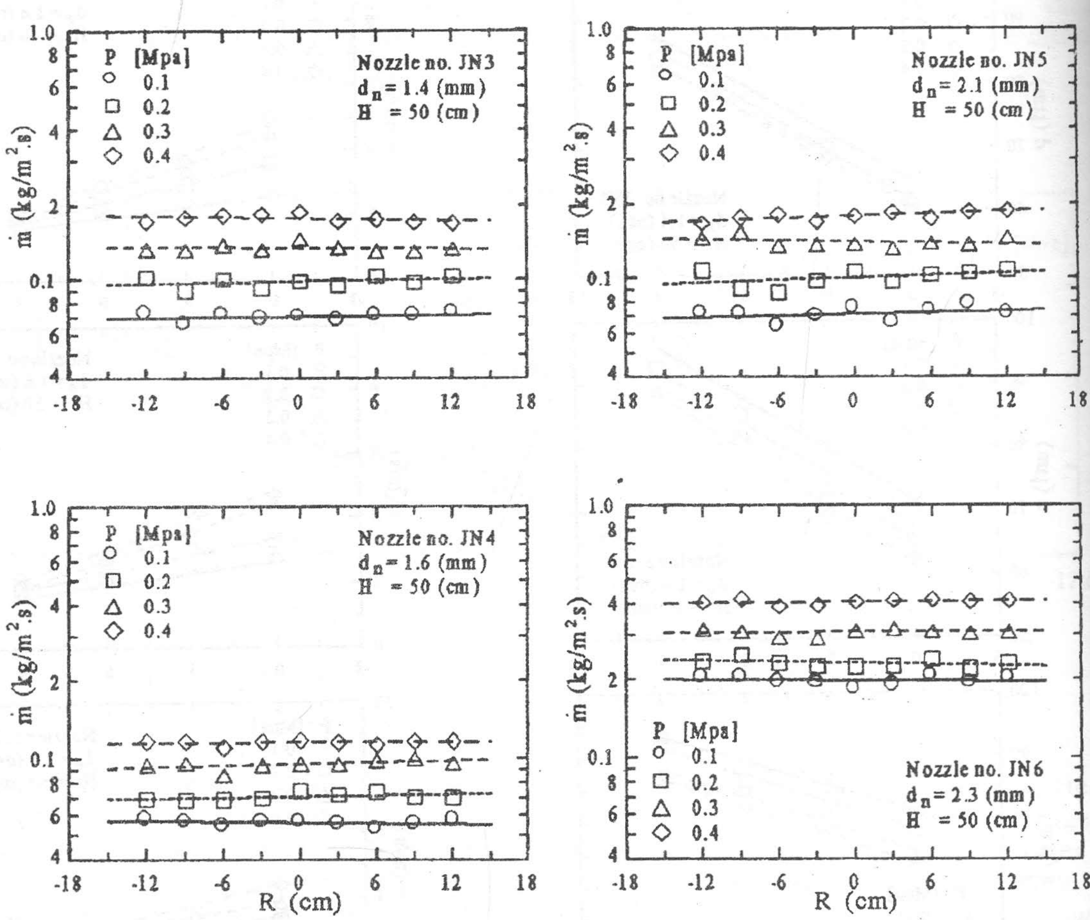

Figure 5 Water masss Velocity radial distribution

Table 1 Characteristics of water spray at 0.5 m downstream of spray nozzle.

Nozzle type	P_s [MPa]	$\dot{m}$ [kg/m².s]	d [μm]	V [m/s]	We [-]
JN3	0.1	0.0672	66.46	2.42	05.54
d_n=1.4 [*mm*]	0.2	0.0936	65.45	3.28	10.02
1/8 KSFS	0.3	0.1358	64.07	4.01	14.66
01565	0.4	0.1766	66.91	4.78	21.75
JN4	0.1	0.0551	73.68	2.46	06.34
d_n=1.6 [*mm*]	0.2	0.0704	74.80	3.13	10.42
1/4 KSFS	0.3	0.0889	70.79	4.01	16.19
0265	0.4	0.1109	67.80	4.41	18.76
JN5	0.1	0.0698	80.09	2.67	08.12
d_n=2.1 [*mm*]	0.2	0.0978	83.92	3.20	12.22
1/4 KSFS	0.3	0.1276	87.04	3.65	16.50
0365	0.4	0.1752	82.50	4.11	19.82
JN6	0.1	0.2014	74.54	3.13	10.39
d_n=2.3 [*mm*]	0.2	0.2292	79.30	3.76	15.94
1/4 KSFS	0.3	0.3140	83.42	4.35	22.45
0465	0.4	0.4158	83.21	5.08	30.55

TEMPERATURE MEASUREMENT

The experimental apparatus used to measure the temperature-time curves of the copper specimen in the transient cooling process is shown in Figure 6. A copper specimen of dimension 0.1×0.1×0.03 m was used as a heat transfer target. Two thermocouples (1 mm diameter, type K) were embedded in the specimen, one at 3 mm from the upper surface and the second at the center. Prior to each experimental run, the upper surface (quenched surface) of the specimen was polished with emery paper to mirror-like surface finish and cleaned with alcohol.

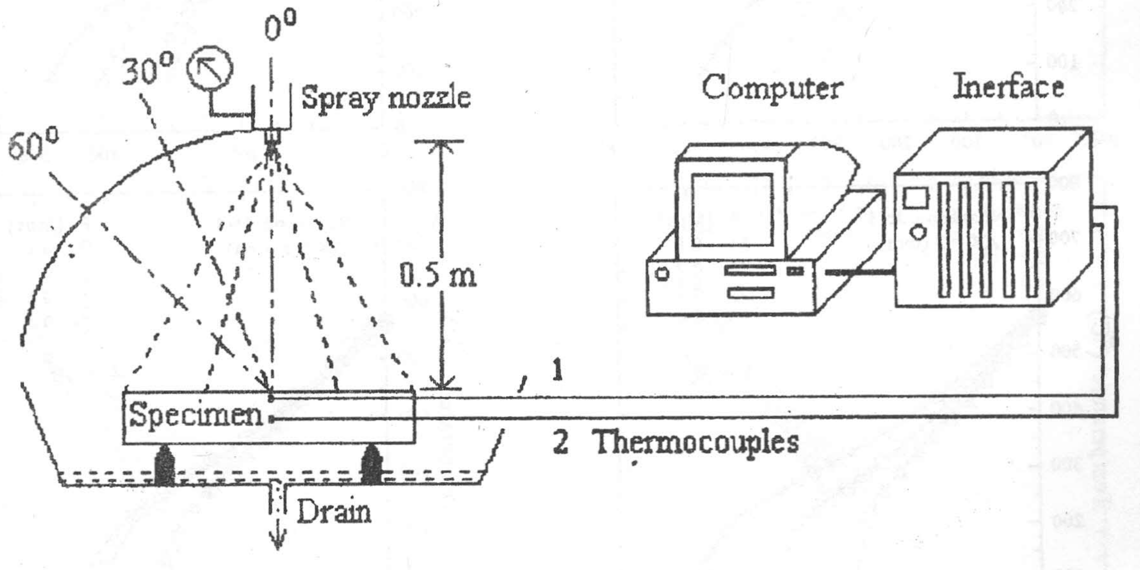

Figure 6 Spray chamber of cooling process

The spray nozzle was directed vertically downward to the heat transfer surface. The impinging angle of the spray was oriented at three positions, perpendicular, 30° and 60° from the vertical direction. The specimen was heated up to 800 °C in a gas furnace. After heating the specimen the spray water is started by set the water flow rate and injection pressure to the atomizing nozzle as desired and then the spray is intercepted. Thereafter, the specimen is clamped to the spray chamber and the cooling process is started. During the cooling process, the temperature of water spray and the temperatures inside the specimen are monitored by a data acquisition system as shown in Figure 6. The temperature-time curves of the cooling process at chosen spray characteristics and spray impinging angle are illustrated in Figures 7 through 10. The cooling time of quenching processes are gradually decreased with increasing injection pressure. But for one set, the cooling time increased with increasing spray angles respect to vertical. These data are used as the input information to a computer program to calculate the surface temperature and heat flux based on the inverse heat conduction model.

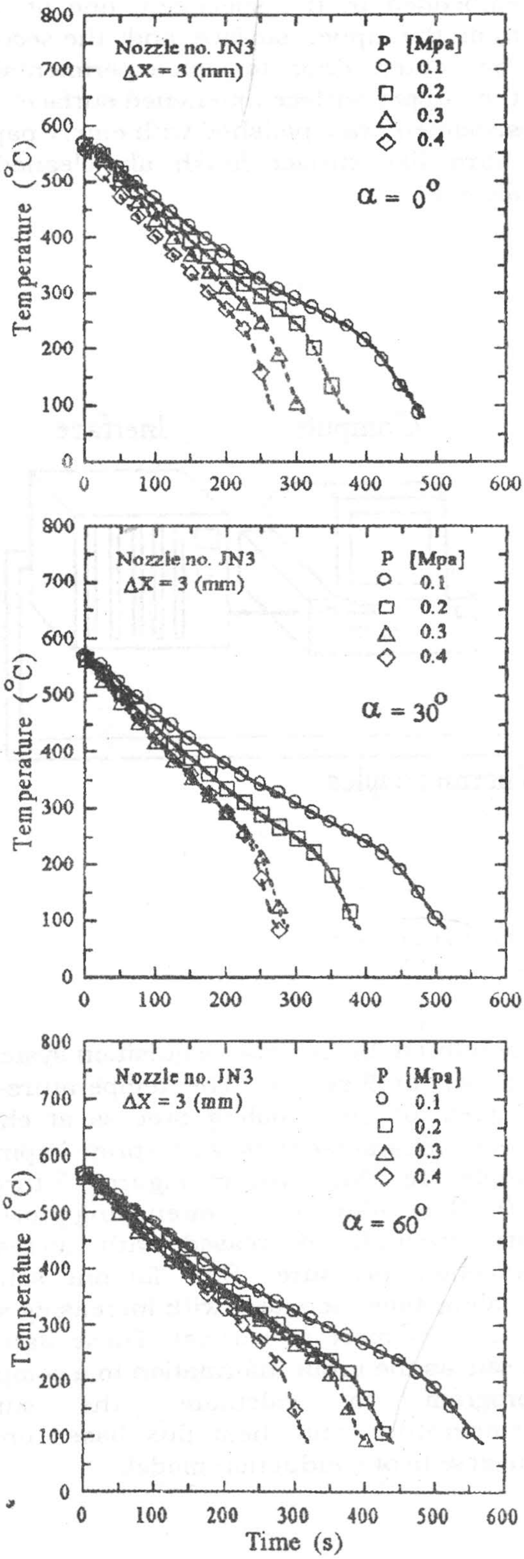

Figure 7 Specimen temperature history-injection from nozzle JN3.

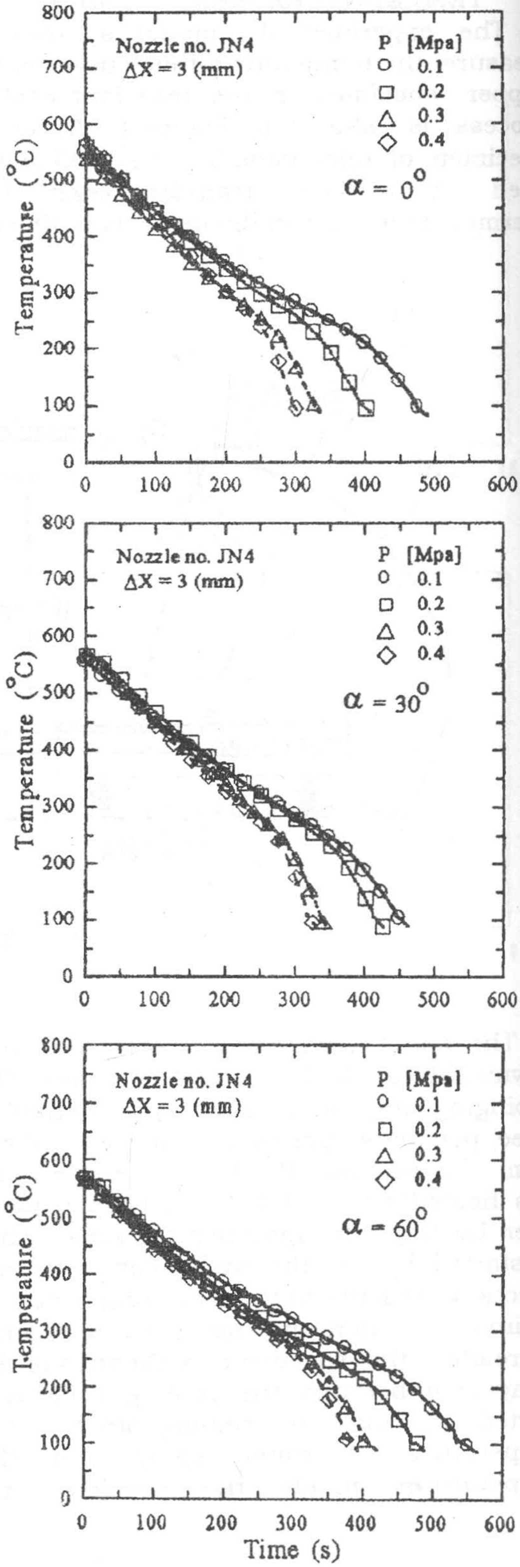

Figure 8 Specimen temperature history-injection from nozzle JN4.

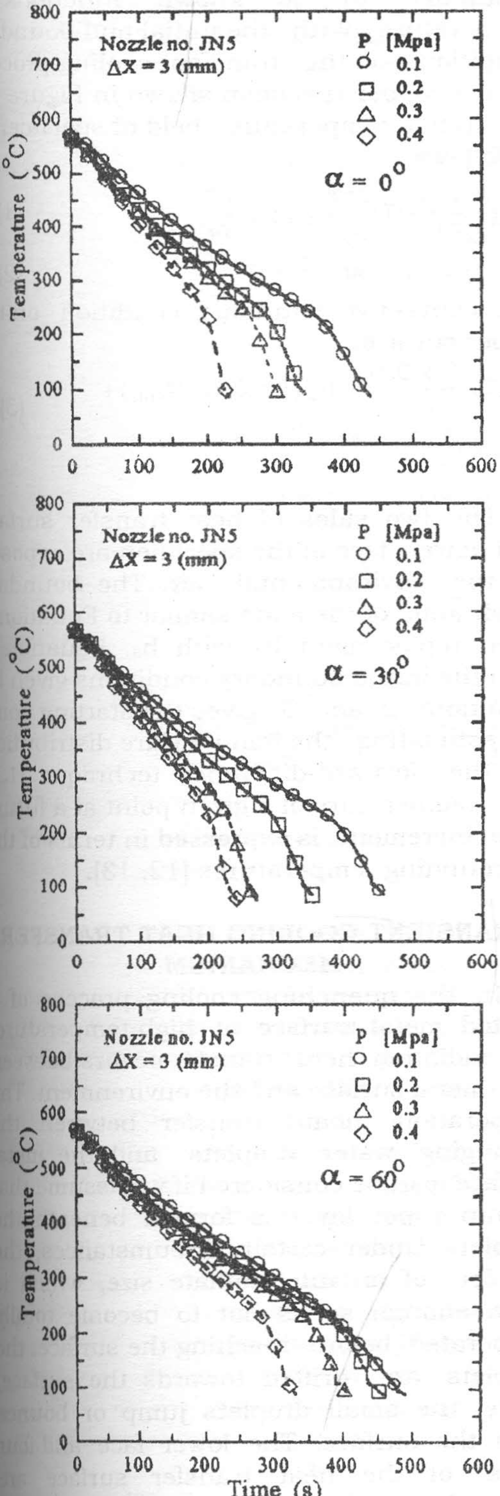

Figure 9 Specimen temperature history-injection from nozzle JN5.

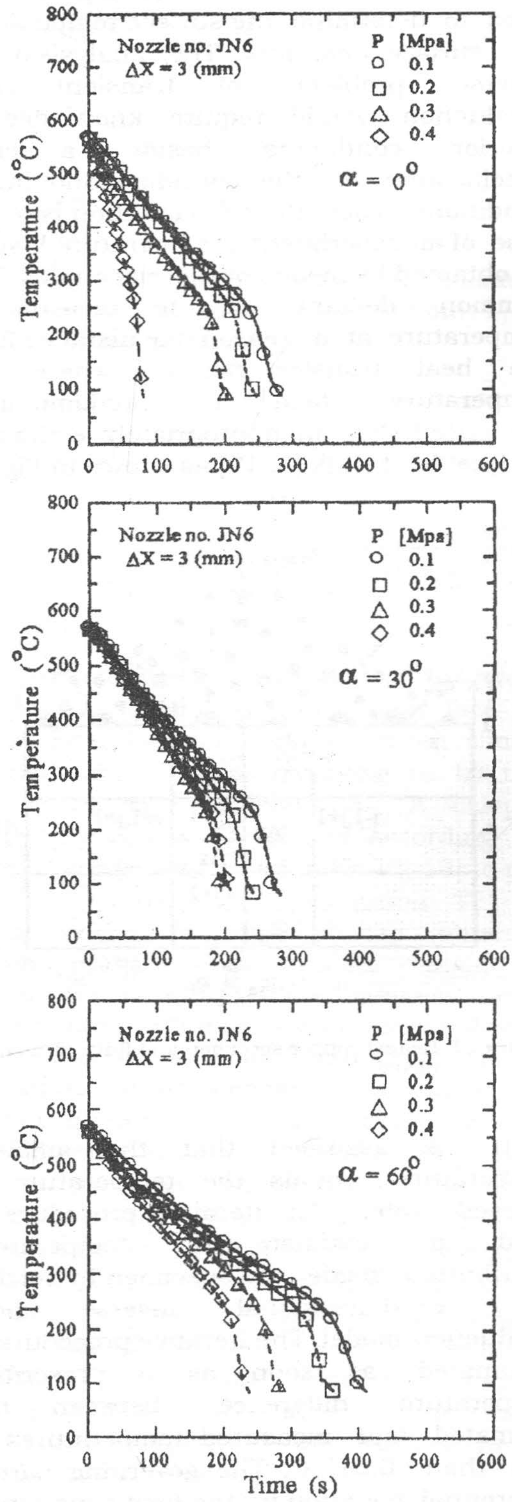

Figure 10 Specimen temperature history-injection from nozzle JN5.

INVERSE HEAT CONDUCTION MODEL

The inverse heat conduction problem is used to determine the surface temperature and surface heat flux. The analysis of the inverse problem of transient heat conduction would require knowledge of interior conditions beside a clear specification of the boundary and initial conditions. The internal condition is in the case of an experimental temperature history is obtained by means of thermocouples. The common demand is to measure a temperature at a reasonable distance from the heat transfer surface where the temperature field is predominantly influenced by an appropriately estimated surface heat flux [3, 12] as shown in Figure 11.

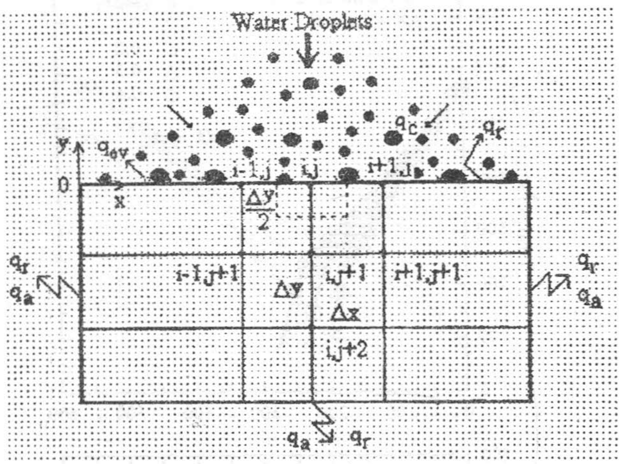

Figure 11 Heated copper specimen and finite element model.

It is assumed that the ambient temperature equals the temperature of sprayed water. An iterative procedure is used to estimate the temperature distribution inside the specimen by solving the two-dimensional inverse heat conduction model. The iterative procedure is terminated as soon as a prescribed temperature difference between the estimated and measured temperatures is less than 0.01 °C. The governing partial differential equation for the heat conduction within the specimen is as follows:

The physical parameters k(T) and c(T) are postulated to be known functions of temperature. With the initial and boundary conditions of the transient cooling process in the copper specimen shown in Figure 11, the initial temperature field of specimen is as follows,

$$k(T)\frac{\partial^2 T}{\partial x^2} + k(T)\frac{\partial^2 T}{\partial y^2} = \rho c(T)\frac{\partial T}{\partial \tau} \quad (1)$$

$$T(x,y) = T_0 \quad \text{at} \quad \tau = 0 \quad (2)$$

The convective boundary condition on the upper surface,

$$-k(T)\frac{\partial T(x,0,\tau)}{\partial y} = h_w(T(x,0,\tau) - T_{sub}) + \sigma\varepsilon(T(x,0,\tau)^4 - T_a^4) \quad (3)$$

The two sides of heat transfer surface and lower face of the specimen are exposed to the environmental air. The boundary conditions of them are similar to Equation 3 after replacement h_w with h_a. Equation 1 with the initial boundary conditions given by Equations 2 and 3 gives the starting point for estimating the temperature distribution by the forward-difference technique [13]. The temperature of a given point at a future time increment is expressed in terms of the surrounding temperatures [12, 13].

TRANSIENT COOLING HEAT TRANSFER MECHANISM

In the quenching cooling process of heated metal surface at high temperature the radiation heat transfer occurs betwee the metal surface and the environment. Th evaporation heat transfer between th impinging water droplets and the meta surface can be considered if we assume tha a thin vapor layer is formed beneath th droplet. Under certain circumstances, th droplet of an intermediate size, which i large enough so as not to become totall evaporated before reaching the surface, th droplets are drifted towards the surface while the small droplets jump or bounc from the surface. The lower face and fou sides of the heat transfer surface ar exposed to the free convection of th surrounding air. The entrained airflov within the spray causes small contributio to the surface heat flux. The total heat transfer from the high temperature metal surface sprayed by the water is due to the contributions from the evaporation, radiation and air convection heat transfer. The contribution of convection heat transfer, q_c, of the entrained airflow within the spray may be quite small and can be neglected [4]. The contribution of radiation heat transfer was estimated as,

$$q_0 = q_w + q_r + q_c \tag{4}$$

$$q_r = \sigma\varepsilon(T_s^4 - T_a^4) \tag{5}$$

The emissivity, ε, of the copper surface was estimated in the previous studies [4~6] and is reported as the following expressions,

$$\varepsilon = \begin{cases} 0.06 & T_s{}^{\circ}C \le 300 \\ 0.06 + 0.002(T_s - 300) & 300 < T_s{}^{\circ}C < 600 \\ 0.7 & T_s{}^{\circ}C \ge 600 \end{cases} \tag{6}$$

The contribution of evaporation heat transfer between the impinging water spray and the heated surface was estimated as,

$$q_w = h_w(T_s - T_{sub}) \tag{7}$$

Where, T_{sub} is the subcooling temperature of the water spray.

METHOD OF SOLUTION

The partial differential equation (given by Equation 1) can be integrated using the finite-difference approximation [13]. The subscript i denotes the x position and the subscript j denotes the y position. A forward-difference technique is used to obtain the temperature after a time increment and Δτ is a function of the previous temperature. The transient energy balance of point i,j can be considered a sum of energy conducted and transferred from the surface to increase the internal energy of the point space as shown in Figure 11. The transient energy equation of the upper surface of the specimen at point i,j can be written as follows:

$$\rho c(T)\frac{\Delta y}{2}\Delta x\frac{\left[T_{i,j}^{\tau+1} - T_{i,j}^{\tau}\right]}{\Delta\tau} = k(T)\frac{\Delta x}{\Delta y}\left[T_{i,j+1}^{\tau} - T_{i,j}^{\tau}\right] + k(T)\frac{\Delta y}{2\Delta x}\left[T_{i-1,j}^{\tau} - T_{i,j}^{\tau}\right] + k(T)\frac{\Delta y}{2\Delta x}\left[T_{i+1,j}^{\tau} - T_{i,j}^{\tau}\right] + h_w\Delta x(T_{sub} - T_{i,j}^{\tau}) + \sigma\varepsilon\Delta x(T_a^4 - T_{i,j}^{\tau}) \tag{8}$$

The temperature equation inside the specimen as an example at point i,j+1 can be written as follows,

$$\rho c(T)\frac{\left[T_{i,j+1}^{\tau+1} - T_{i,j+1}^{\tau}\right]}{\Delta\tau} = \frac{k(T)}{\Delta x^2}\left[T_{i+1,j+1}^{\tau} + T_{i-1,j+1}^{\tau} - 2T_{i,j+1}^{\tau}\right] + \frac{k(T)}{\Delta y^2}\left[T_{i,j}^{\tau} + T_{i,j+2}^{\tau} - 2T_{i,j+1}^{\tau}\right] \tag{9}$$

The temperature equations of the two sides (left and right) and the lower face of the surface can be easily written similar to Equation 8 after replacing h_w by the air convection coefficient h_a. A calculation program was developed according to the procedure explained in [2, 12, 13] to predict the temperature distribution $T^{\tau+1}$. The procedure is repeated to obtain the temperature distribution inside the specimen. The predicted temperature at the assumed value of h_w was compared with the measured value at 3 mm from the upper surface of the specimen. The value of h_w was re-adjusted by the iteration method to give a difference of 0.01 °C between the measured and predicted temperatures. The time step Δτ was varied from 10^{-4} to 10^{-5} s. The increments Δx and Δy were kept equal to 1 mm. The temperature distribution within the specimen before water spray was calculated with air convection of h_a = 8.72 W/(m². K). The calculation steps are repeated at each interval time until the surface temperature and surface heat flux are readily obtained.

RESULTS AND DISCUSSION

Figures 7 through 10 show the measured temperature variation at 3 mm inside the specimen. At the vertical impinging condition, the increase of droplet mass velocity accomplished by increasing water supply pressure decreases the cooling time of specimen. But for inclined impingement spray at the same spray characteristics, the cooling time is increased for spray angle of 30° and 60°. To validate the effect of spray parameters on the cooling time, the cooling average temperature of the specimen is taken as the temperature difference between the initial temperature (the recorded temperature at starting quench process) and saturation temperature of water, ΔT_{av} = 450 °C. The value of the cooling time corresponding to the cooling average temperature is illustrated in Figure 12. Quite naturally, the cooling time is closely related to the spray parameters. It is clear that the cooling time decreases with the increase of the mass velocity, droplet impinging velocity and droplet size. Also, the cooling time increases with the increase of impinging spray angle, α, from 0 to 60°. It is shown in Figure 12, at lower values of mass velocity 0.143 kg/m². s, droplet impinging velocity 3.28 m/s, and droplet size 65 μm that the cooling time is shorter at α = 30° than at the vertical α = 0°. This may be due to the effect of the droplet interaction and collision upon the heat transfer surface, and the decrease of vertical component of the droplet impinging velocity.

Boiling Curve of Transient Cooling Process

Typical relationships between the surface heat flux and surface temperature at different spray parameters are illustrated in Figures 13 through 16. It is observed from these figures that the surface heat flux is very sensitive to the spray parameters and always has positive effect with impinging water mass velocity. Obviously, the trend of the boiling curves has three distinguished regions, namely, the nucleate, transition and film boiling. The water mass velocity, droplet size, droplet impinging velocity and impinging spray angle are playing important roles on the heat transferred from the heated surface to the water spray.

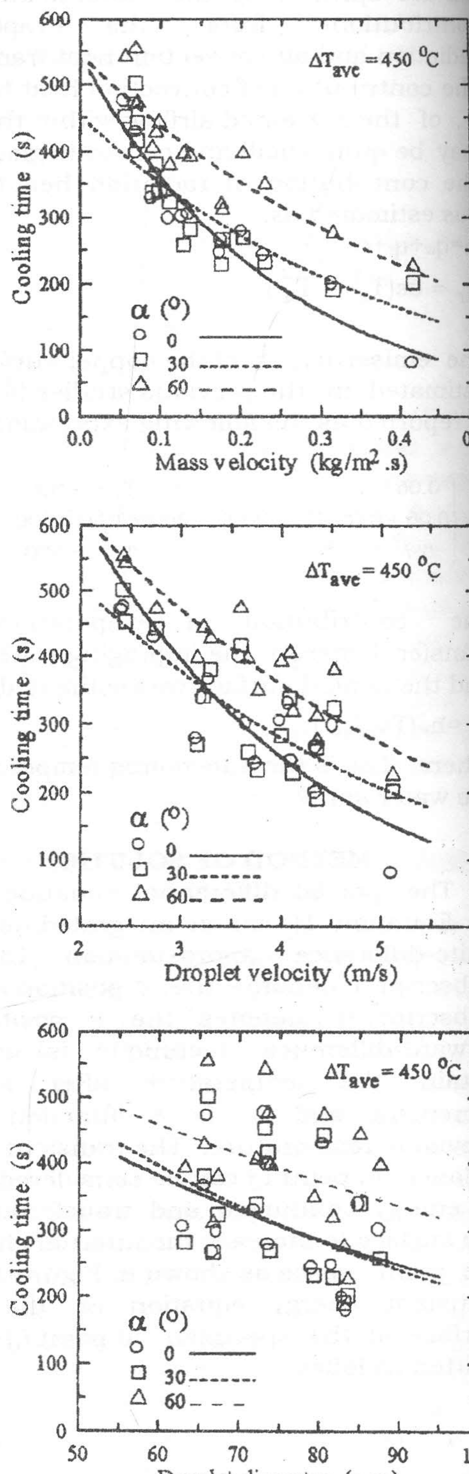

Figure 12 Effect of spray characteristics on the rate of cooling time.

Throughout the experimental runs at high surface temperature, the water droplets did not wet the surface and bounce from the surface. The droplets are reflected towards the surface edges as rubber spheres isolated by a thin vapor layer. At this moment, the rates of temperature decrease with time are small and vapor generation is not observed, (film boiling region). At moderate surface temperature about 280 °C, the vapor generation is started and an audible noise is heard, (transition boiling region). The rate of temperature decrease is increased and the vapor generation attains a maximum (maximum heat flux). Thereafter, the water droplets wet the surface and flatten out into small batches, which form a thin liquid film upon the surface, (nucleate boiling region). The evaporation will take place on the outside surface of the flattened droplet during a short time before it completes evaporation [11].

The transient cooling curves in Figures 13 to 16 indicate that the surface heat transfer capability increases with the water mass velocity. Since the droplet impinging velocity and diameter are determined from a chosen mass velocity, it is logical to conclude that the droplet diameter and velocity influence the surface heat flux. Also, the effect of spray impinging angle on the surface heat flux could be seen. The surface heat flux decreases with increasing the spray angle from the vertical. It is observed that the Leidenfrost temperature (temperature limit between film and transition boiling) occurred at 160 to 180 °C above the saturation temperature. Also, the maximum heat flux occurred at 40 to 60 °C above the saturation temperature as shown in Figures 13 to 16. It can be concluded that the spray parameters have little effect on the Leidenfrost temperature.

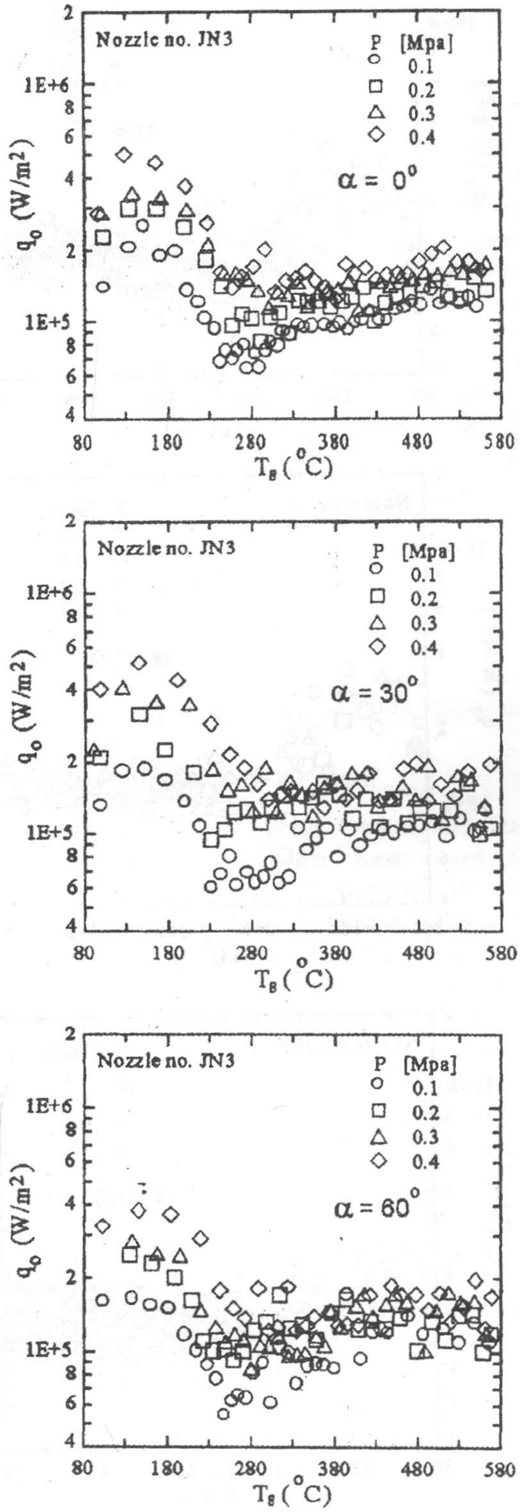

Figure 13 $q_\cdot$ versus T_s for nozzle JN 3

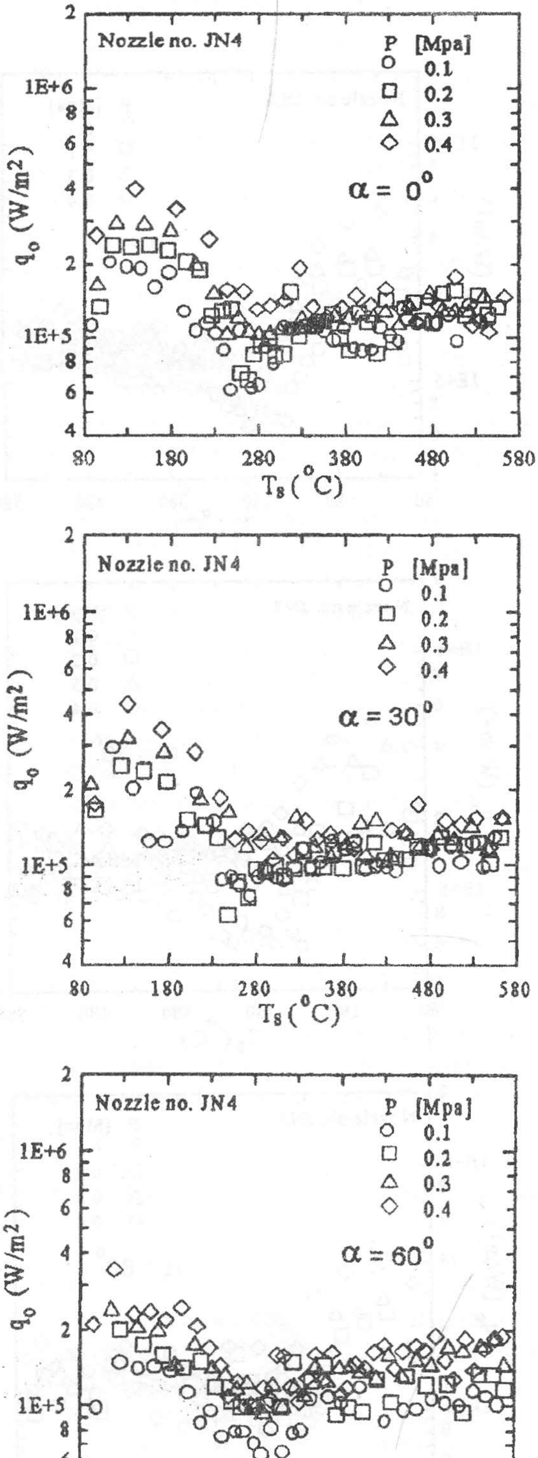

Figure 14 q_o versus T_s for nozzle JN 4

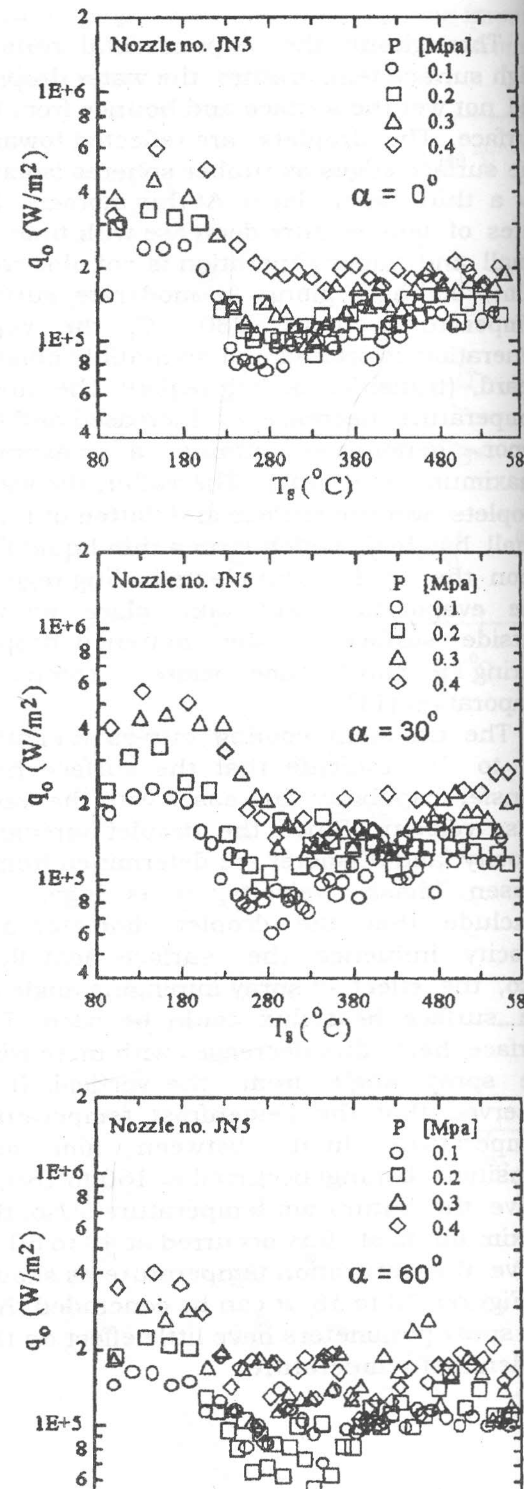

Figure 15 q_o versus T_s for nozzle JN 5

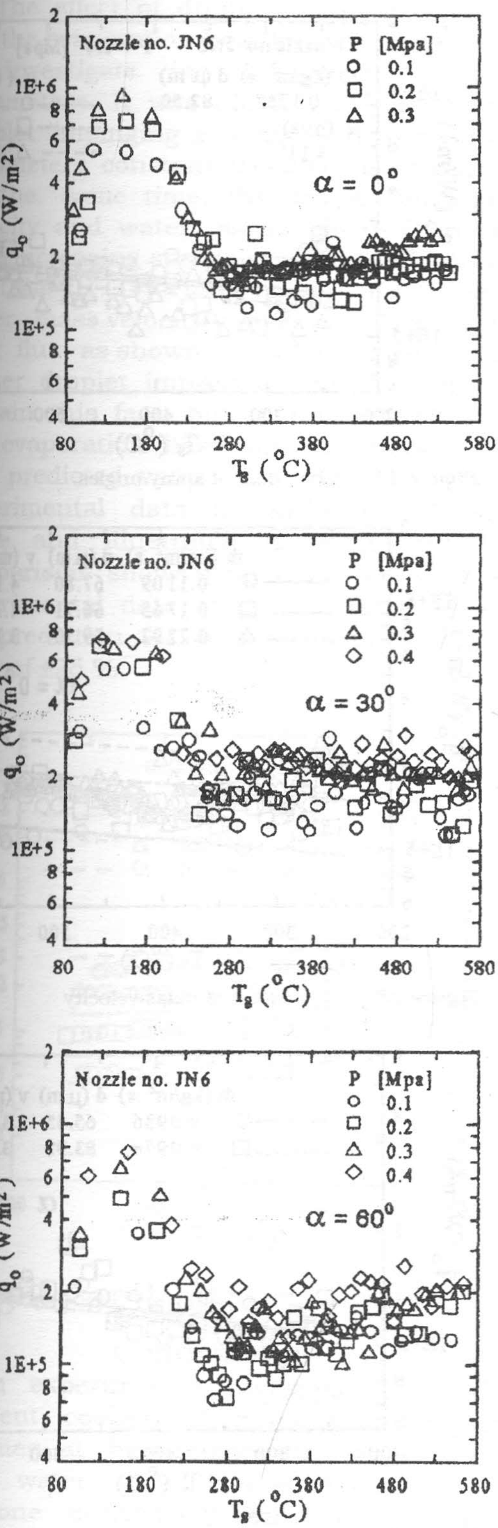

Figure 16 q_o versus T_s for nozzle JN 6

Correlation of Evaporation Heat in Film Boiling Region.

The analysis and correlation of the evaporation heat flux in terms of the experimental tested variables were performed. The contribution of radiation heat flux is subtracted from the surface heat flux in film boiling region to obtain the evaporation heat flux. Division of the evaporation heat transfer data by the water mass velocity and vaporization heat yields a dimensionless value (effectiveness of heat transfer surface). Four thousand experimental data points were correlated in dimensionless groups with the spray parameters and thermodynamic properties of liquid and vapor. A correlation of the evaporation heat transfer in film boiling region for vertical impinging water spray has been obtained as follows,

$$\frac{q_w}{m\lambda_m} = 1.09\left(\frac{gk_v\Delta T_{sup}d}{V^2\mu_v h_{fg}}\right)^{0.024}\left(\frac{1}{We}\right)^{0.324} \qquad (10)$$

Where, λ_m denotes the vaporization heat and is defined as:

$$\lambda_m = c_{pl}\Delta T_{sub} + h_{fg} + c_{pv}\Delta T_{sup} \qquad (11)$$

A comparison between the experimental data of the evaporation heat and the prediction values by Equation 10 was conducted. It was found that a 42% of the predicted values are less than by an error ±20%, with 74% of the predicted values are less than an error of ±50% from the experimental data. The effect of spray impinging angle can be interpreted as the dimensionless ratio of the angle to a vertical 90°. Vertical and inclined experimental evaporation heat transfer data of 13 thousand points were correlated with an error of ±20% for 49% of tested data. And for 87% of the tested data the error is ±50 %. A generalized correlation of the evaporation heat transfer for vertical and the inclined impinging spray in range of α from 0 to 60° and We ≤ 30 has been obtained in the following form:

$$\frac{q_w}{\dot{m}\lambda_m} = 1.28\left(\frac{90-\alpha}{90}\right)^{0.129}\left(\frac{k_v \Delta T_{sup}}{\mu_v h_{fg}}\right)^{0.064}\left(\frac{1}{We}\right)^{0.448} \quad 0^o \le \alpha \le 60^o \tag{12}$$

To confirm the validity of the generalized correlation of evaporation heat transfer in film boiling region, Equations (12), the effect of spray parameters are investigated and compared with the prediction. The range of spray parameters cited, is water mass velocity of 0.05 to 0.42 $kg/m^2.s$, droplet impinging velocity of 2.42 to 5.11 m/s, droplet size of 63 to 88 μm and spray impinging angle of 0 to 60°. The temperature of impinging water is 25 °C and the surface temperature from 750 to 90 °C.

The effect of spray impinging angle on the evaporation heat flux is illustrated in Figure 17. It is seen that the evaporation heat flux decreases with the increase of the spray impinging angle with respect to the vertical. Thus far, the vertical component of droplet velocity is decreased in the case of inclined impinging spray than in the vertical case. So, the contact area between water droplets and heat transfer surface decreases due to the Weber number causing a reduction in the evaporation heat flux. Figure 18 shows the effect of mass velocity of water on the evaporation heat flux. In this plot, the increase of mass velocity of water has positive effect and did exhibit a little effect on evaporation heat flux in film boiling region. The effect of droplet diameter on evaporation heat flux is shown in Figure 19. In this graph, the mass velocity of water and impinging velocity of droplets are nearly constant, but the droplet diameter differs by about 20 μm. It is seen that the evaporation heat flux decreases with the increase of droplet diameter.

On the other hand, for smaller droplet diameter, the heat transfer surface is struck by a large number of droplets per unit of time and the evaporation heat flux goes up.

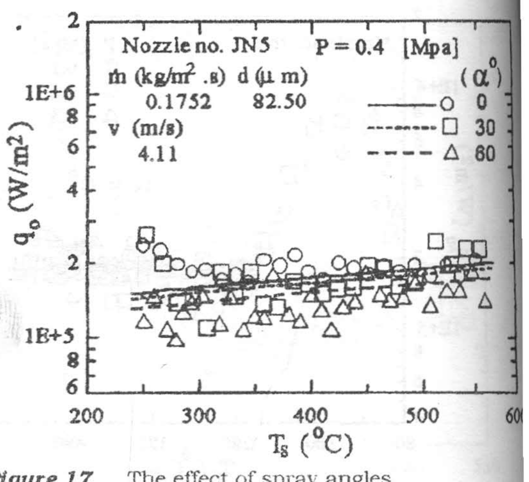

Figure 17 The effect of spray angles.

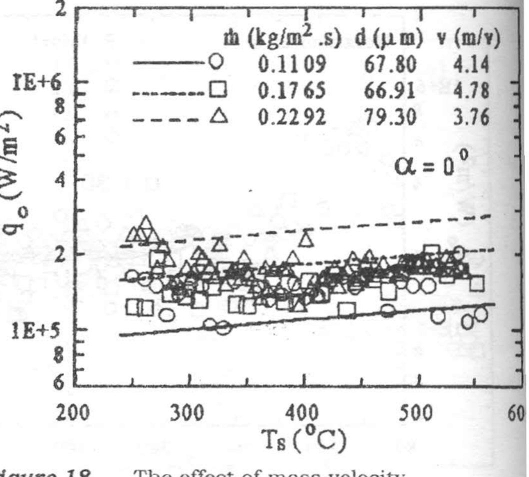

Figure 18 The effect of mass velocity

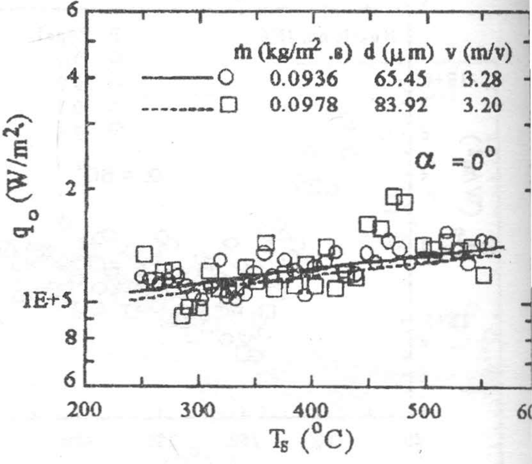

Figure 19 The effect of droplet diameter.

The effect of droplet impinging velocity on the evaporation heat flux was impossible to investigate in this range of spray parameters. It was difficult to change the droplet impinging velocity and keep other parameters constant especially for pressure. At the same time, the droplet impinging velocity and water mass velocity increases with increasing spray pressure as illustrated in Table 1. Obviously higher impinging water mass velocity causes a higher surface heat flux as shown in Figures 13 to 16. The higher droplet impinging velocity can also explain this fact, but it has little effect on the evaporation heat flux. A comparison of the predicted values by Equation 12 and experimental data in Reference 15 were made and illustrated in Figure 20. The comparison shows good agreement between experimental data of surface heat flux and the prediction for vertical spray within an error of ±25 %.

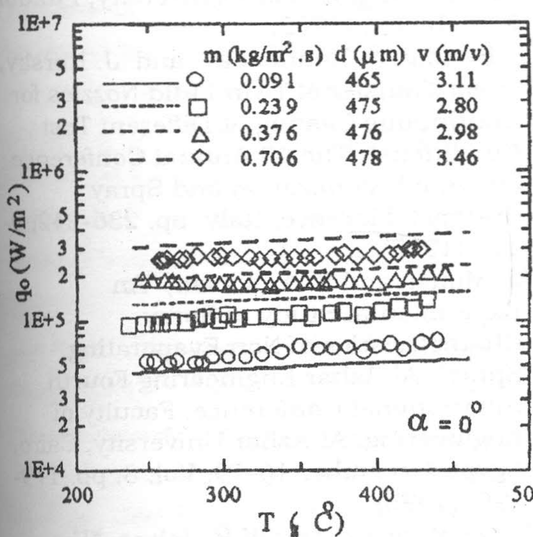

Figure 20 Comparison with experimental data [15].

CONCLUSIONS

An experimental investigation of the transient cooling of a horizontal copper specimen at high temperature up to 800 °C using water spray has been carried out. Full-cone nozzles with orifice diameter from 1.4 to 2.3 mm were used and the spray characteristics as droplet size, droplet impinging velocity and water mass velocity at various heights downstream of the spray nozzle were measured. The temperature history at two locations inside the copper specimen was recorded with a data acquisition system and the surface temperature and heat flux was estimated by solving an inverse heat conduction model. An iteration method is employed to estimate the temperature distribution inside the specimen by assuming the surface heat transfer coefficient and adjust it to give a temperature difference of 0.01°C between the measured and calculated values. The boiling curves of transient cooling were obtained in the ranges of water mass velocity of 0.05 to 0.42 kg/m^2.s and Weber number ≤ 30.

The results are summarized as follows:

1. The evaporation heat flux is strongly influenced by the water mass velocity, and increases when the water mass velocity is increased.
2. The droplet impinging velocity and size have small effects on the evaporation heat flux in the film-boiling region. A smaller droplet size causes a better evaporation heat flux due to the increase in droplet number per unit time. The effect of impinging velocity was not observable at high water mass velocity.
3. The evaporation heat flux decreases with the increase of the impinging spray angle with respect to the vertical. The evaporation heat flux decreases with the decrease of Weber number, due to the decrease of Weber number in case of inclined spray than in the vertical case.
4. A general correlation equation for evaporation heat transfer in film boiling region has been developed for vertical and inclined water sprays.

NOMENCLATURE

c	:	metal specific heat [J/(kg.K)]
c_p	:	liquid specific heat [J/(kg.K)]
d	:	droplet diameter [m]
d_n	:	nozzle diameter [m]
h	:	heat transfer coefficient [W/(m^2.K)]
h_{fg}	:	latent heat of evaporation [J/kg]
k	:	thermal conductivity [W/(m.K)]

$\dot{m}$: mass velocity [kg/(m^2.s)]
P_s : supply pressure [MPa]
q : heat flux [W/m^2]
q_o : total surface heat flux [W/m^2]
T : temperature [K]
ΔT_{sup}: surface superheating T_s-T_{sat} [K]
ΔT_{sub}: water subcooling T_{sat}-T_l [K]
V : impinging velocity [m/s]
We : Weber number ($\rho_l v^2 d/\sigma_l$) [-]
x : horizontal direction [m]
y : vertical direction [m]
α : spray impinging angle [°]
ε : emissivity [-]
λ_m : vaporization heat [J/kg]
μ : viscosity [kg/(m.s)]
ρ : density [kg/m^3]
σ : Stefan-Boltzman constant [W/(m^2.K^4)]
σ_l : liquid surface tension [N/m]
τ : time [s]
$\Delta\tau$: time step [s]

Subscript

A : Environmental air
Av : Average
C : Air convection
L : Liquid
R : Radiation
Sat : Saturation
Sub: Subcooling
Sup: Superheating
S : Surface
V : Vapor
W : Evaporation
0 : Initial condition

REFERENCES

1. L. C. Pais, E. T. Chow and Mahefkey, "Surface Roughness and its Effect on the Heat Transfer Mechanism in Spray Cooling, Heat Transfer in High Energy/High Heat Flux Applications", HTD-Vol. 119, pp. 51-59, 10-15, (1989).
2. T. I. Sabry M. Mousa and H. Yoshida, "Studies on the Spray Cooling of Hot Surfaces", ICLASS-94, Rouen, France, pp. 891- 898, (1994).
3. M. Horsky, V. Raudensky, Dumek and L. Bendig, "Experimental Study of Heat Transfer in Process of Cooling by Twin Fluid Nozzle", ICLASS-94, Rouen, France, pp. 1055-1061, July 1994.
4. Y. Ito, M. Takata, Mousa and H. Yoshikai, "Studies on the Water Cooling of Hot Surfaces (Experiment of Spray Cooling)", Memoirs of the Faculty of Engineering, Kyushu University, Fukuoka 812, Japan, Vol. 51, No. 2, pp. 119-144, (1991).
5. Y. Ito Takata and M. Mousa, "Studies on the Water Cooling of Hot Surfaces (Analysis of Spray Cooling in the Region Associated with Film Boiling)", JSME International Journal, Series II, Vol. 35, No. 4, pp. 589-598, (1992).
6. M. Mousa, Y. Ito and Y.Takata, "Studies on the Spray Cooling of Hot Surfaces", Al-Azhar Engineering Second International Conference, Faculty of Engineering, Al-Azhar University, Cairo, Egypt, December 21-24, Vol. VII, pp. 119-133, (1991).
7. M. Mousa, "Spray Cooling of Hot Surfaces", Ph. D. Thesis, Faculty of Engineering, Kyushu University, Fukuoka 812, Japan, (1992).
8. L. Bendig, N. Raudensky, and J. Horsky, "Heat Transfer of Twin Fluid Nozzles for Continuous Casting at Different Test Conditions", The 13 Annual Conference on Liquid Atomization and Spray Systems, Florence, Italy, pp. 236-242, 9-11, (1997).
9. M. Mousa and S. A. Wilson, "An Experimental Study of Spray Characteristics of Non Evaporating Spray", Al-Azhar Engineering Fourth International Conference, Faculty of Engineering, Al-Azhar University, Cairo, Egypt, December 16-19, Vol. 8, pp. 179-196, (1995).
10. M Dombrowski and W.R. Johns, "The aerodynamic Instability and Disintegration of Viscous Liquid Sheets", Chemical Engineering Science, Vol. 18, (1963).
11. D. Moreau and J. M. Buchlin, "An Experimental Study of Liquid Sprays Induced by A Full Cone Nozzle", ICLASS-94, Rouen, France, pp. 366- 373, July (1994).

12. J. V. Beck, B. Blackwell and R. S. Charles, "Inverse Heat Conduction", Wiley, (1985).
13. J.P. Holman, "Heat Transfer", Sixth Edition, pp.158-164, (1986).
14. Lee Z. H. Yang and Y. Hsyua, "Cooling of a heated Surface by Mist Flow", Journal of Heat transfer, Vol. 116, pp. 167-172, (1994).
15. S. C. Yao and K. J. Choi, "Heat Transfer Experiments of Mono-Dispersed Vertically Impacting Sprays", Int. J. Multiphase Flow, Vol. 13, No. 5, pp. 639-648, (1987).

Received September 20, 1998
Accepted April 22, 1999

التبريد الفجائى لسطح معدنى ساخن برش ماء

موسى محمد محمد موسى
قسم هندسة القوى الميكانيكية، كلية الهندسة جامعة المنوفية

ملخص البحث

يتناول البحث تجارب لانتقال الحرارة فى الطور الغير مستقر لسطح معدنى ساخن من النحاس على شكل متوازى مستطيلات ٠,١ × ٠,١ × ٠,٠٣ م ، تم تسخين عينة النحاس فى فرن غاز حتى درجة حرارة ٧٥٠ °م ثم إخراج العينة ووضعها فى غرفة رش الماء بواسطة نظام للضخ وأبواق رش بقطر يتراوح من ١,٤ حتى ٢,٣ مم لتزرير الماء إلى قطرات عند ضغوط رش من ٠,١ حتى ٠,٤ ميجابسكال وتسجيل درجات الحرارة مع الزمن باستخدام دائرة معلومات وحاسب آلى ، وتم تثبيت ازدواج حرارى فى عينة النحاس على بعد ٣ مم من السطح داخل عينة المعدن وعند مركز العينة ، والازدواج الحرارى متصل بدائرة معلومات وحاسب آلى واستخدام برنامج قياسات لتسجيل درجات الحرارة مع الزمن ، وتم دراسة تأثير معدل رش الماء على السطح وقطر وسرعة القطرات وزاية ميل الرش على الرأسى على معدل انتقال الحرارة من السطح الساخن إلى قطرات الماء ابتداء" من درجة حرارة ٦٥٠ °م حتى ٨٠ °م فى ظروف الضغط الجوى.

واستخدمت معادلة انتقال الحرارة بالتوصيل للطور الغير مستقر فى بعدين كنموذج رياضى لحساب معدل انتقال الحرارة من السطح المعدنى إلى قطرات الماء ، وباستخدام تقنيات الطرق العددية لحل المعادلات التفاضلية أمكن حل النموذج الرياضى عند الظروف المحيطة للسطح المعدنى وظروف رش مختلفة، ثم مقارنة النتائج المحسوبة لتوزيع درجات الحرارة داخل العينة بالنتائج المقيسة وأمكن الحصول على معامل انتقال الحرارة بين السطح المعدنى الساخن وقطرات الماء عندما يكون الفرق بين درجة الحرارة التى تم قياسها والمحسوبة أقل من ٠,٠١ °م ، وقد وجد أن معدل انتقال الحرارة بالتبخير يتأثر بقوة ويزيد بزيادة معدل رش الماء على السطح الساخن ، وأن قطر القطرات وسرعة اصطدامها بالسطح الساخن له تأثير طفيف على معدل انتقال الحرارة بالتبخير، أما القطرات ذات القطر الصغير تسبب تبريدا" أفضل للسطح لزيادة عدد القطرات لكل وحدة مساحة ، أما سرعة اصطدام القطرات بالسطح الساخن عديمة التأثير عند معدلات رش عالية ، وأن معدل انتقال الحرارة بالتبخير أفضل عند زاوية رش ٣٠ °. وهذا التأثير نتيجة تصادم القطرات على السطح الساخن وتكوين قطرات أكبر أو تكسير القطرات الكبيرة، وتم الحصول على معادلة عملية لحساب معدل انتقال الحرارة بالتبخير للرش الرأسى والرش المائل بطريقة المربعات الصغرى كدالة فى خصائص الرش للقطرات ودرجة حرارة تحميص السطح الساخن، وكانت المقارنة بين النتائج العملية والمحسوبة مرضية جدا" وكان متوسط الخطأ بين النتائج العملية والمحسوبة يتراوح عند ± ٢٥ %.